2009

Neonatal CPR: room at the top—a mathematical study of optimal chest compression frequency versus body size

Charles F. Babbs
Purdue University, babbs@purdue.edu

Andrew Meyer

Vinay Nadkarni

Neonatal CPR: room at the top—a mathematical study of optimal chest compression frequency versus body size

Charles F. Babbs[a,b], Andrew Meyer[c], and Vinay Nadkarni[d]

[a] Department of Basic Medical Sciences, and the Weldon School of Biomedical Engineering, Purdue University

[b] Indiana University School of Medicine

[c] Department of Neonatology, Children's Hospital of Philadelphia

[d] Department of Anesthesia and Critical Care, Children's Hospital of Philadelphia

Address for correspondence and proofs:
Charles F. Babbs, MD, PhD
1426 Lynn Hall
Purdue University
West Lafayette IN 47907-1246, USA
E-mail: babbs@purdue.edu
Voice: 765-496-2661, Fax: 765-494-0781

Abstract

Objective: To explore in detail the expected magnitude of systemic perfusion pressure during standard CPR as a function of compression frequency for different sized people from neonate to adult.
Method: A 7-compartment mathematical model of the human cardiopulmonary system—upgraded to include inertance of blood columns in the aorta and vena cavae—was exercised with parameters scaled to reflect changes in body weight from 1 to 70 kg.
Results: Maximal systemic perfusion pressure occurs at chest compression rates near 60, 120, 180, and 250 per minute for subjects weighing 70, 10, 3, and 1 kg, respectively. Such maxima are predicted by analytical models describing the dependence of stroke volume on pump filling time in the presence of blood inertia. This mathematical analysis reproduces earlier experimental results of Fitzgerald et al. in 10 kg dogs.
Conclusions: Fundamental geometry and physics suggest that the most effective chest compression frequency in CPR depends upon body size and weight. In neonates there is room for improvement at the top of the compression frequency scale at rates > 120/min. In adults there may be benefit from lower compression frequencies near 60/min.

Key words: Basic life support (BLS); Cardiopulmonary resuscitation (CPR); Coronary perfusion pressure; External chest compression (ECC); Mathematical model

1. Introduction

Without adjuncts such as interposed abdominal compression[1, 2], the major variables that can be adjusted during basic life support to improve artificial circulation include the chest compression depth and the chest compression frequency. In infants and neonates, current guidelines[3] recommend external compression to a depth of 33% of the chest diameter, which is relatively greater than that recommended for adults (about 20% of chest diameter). Further, our recent analysis of CT images of neonates (Online Supplement 4) reveals that with 33% compression depth one quarter of patients would experience maximal or over-compression of the mediastinum, completely flattening the heart within the anatomic space available between the sternum and the spine. If compression depth were increased further to 50% of chest diameter, there would be over compression of the heart in nearly all neonates. It seems therefore that there is little room for improvement of neonatal CPR in the domain of compression depth.

The optimal rate or frequency of chest compression in neonates remains uncertain[4-6]. Since natural heart rates in neonates are in the range of 120-160 beats/min, we wondered if increasing chest compression frequency in neonatal patients might have the potential to boost artificial cardiac output compared to recommended compression frequencies, which are based largely on experimental work in animal models larger than neonates. In

particular, we wondered if there might be a more sophisticated way to extrapolate animal and adult human data to patients of very small size, based on fundamental principles of mathematics, physics, and biology. This paper is dedicated to the proposition that such an extrapolation method is possible and indeed confirms the experiment of evolution for naturally beating hearts that faster rates are more effective and appropriate for smaller animals.

2. Theory

2.1 Scaling

Scaling rules in biology describe the structural and functional consequences of changes in body size among geometrically similar organisms[7]. Certain relationships between a representative linear dimension of an animal, L, a particular cross-section, A, and body weight, W, are valid for animals of similar body shape. For example, lean body weight scales with the cube of any particular linear dimension, and the cross sectional area of blood vessels scales with the square of the linear dimension.

To model effects of compression frequency in CPR over a wide range of body sizes, we need to know the scaling rules for relevant cardiovascular parameters. Vascular resistance is the ratio of perfusion pressure across a vascular bed to blood flow through the vascular bed. Normal arterial blood pressure and systemic perfusion pressure are relatively constant for humans of different body size from newborn to adult. Basal metabolic rate, and in turn oxygen consumption, scale approximately with body surface area—the predominate site of heat loss. The scaling of cardiac output with body surface area has lead to the concept of cardiac index, or forward blood flow per square meter of body surface area[8]. Since surface area is proportional to L^2 and weight is proportional to L^3, the body surface area is proportional to the 2/3 power of body weight, $W^{2/3}$. In turn, blood flow or normal resting cardiac output is also proportional to $W^{2/3}$. Thus vascular resistance scales as pressure/flow, or $1/W^{2/3} = W^{-2/3}$, where pressure is constant across scales. So for vascular resistance, R, we can write for an appropriate constant, k_1,

$$R = k_1 W^{-2/3} . \qquad (1a)$$

The compliance, C, of blood vessels is a function of vessel radius, $C = 2\pi L r^3/(Eh)$, where L is the length of the tube, r is the radius, E is Young's modulus of elasticity of the wall material, and h is the thickness of the tube[9]. For people of different size, r and h are proportional to L. This means that compliance scales as L^3 or the first power of body weight, W. Thus for vascular compliance we can write for an appropriate constant, k_2,

$$C = k_2 W . \qquad (1b)$$

To change parameters from one body weight to another, suppose that we have a parameter, X, (such as L, R, or C) that scales with weight, W, according to the power function

$X(W) = kW^a$, where k and a are constants and W is weight in kg. The reference adult body weight is 70 kg. Then $k = X(70)/70^a$, so the parameter value for any arbitrary weight, W, in terms of the value for a 70 kg adult is

$$X(W) = X(70)\left(\frac{W}{70}\right)^a . \qquad (2)$$

In this way it is possible to scale theoretical models of the cardiovascular system for persons of different size from full sized adults to tiny babies, beginning with a standard textbook model for a 70 kg adult.

2.2 A working hypothesis

In a comprehensive study of the effects of compression frequency during cardiac arrest and CPR in medium sized dogs, Fitzgerald and coworkers[10] found that effects of compression timing variables are explained largely by limitations of pump filling and emptying, with the pump filling terms being dominant. As long as the fraction of cycle time during which the pump input valve is open is greater than the time required for adequate pump filling, then there is cardiac output (compression rate × stroke volume) to be gained by increasing the compression frequency. However, as compression frequency increases further, time for pump filling decreases. Then the pump fills only partially, so stroke volume decreases. In turn, cardiac output levels off and may even diminish at faster compression rates. This general principle was confirmed experimentally and applies either to the cardiac pump mechanism or the thoracic pump mechanism of CPR[11], as well as to the naturally beating heart. Accordingly, to understand compression frequency effects in CPR, we decided to focus on pump filling.

To describe filling-related tradeoffs quantitatively, imagine an exceedingly simple two compartment model shown in Figure 1(a) in which the elastic central venous reservoir, C_v, denoting the venae cavae and right atrium, is connected to the input reservoir of the chest pump, C_p, denoting the right ventricle, by a low resistance pathway that includes the one-way tricuspid valve. A column of venous blood with mass density, ρ, cross sectional area, A, and length, L, flows into the right ventricle (C_p) under the influence of axial pressure difference between C_v and C_p during a particular fraction, σ, of total compression cycle time, such as 1/3rd. For this simple model, as shown in Online Supplement 1, the compression frequency f_{max} for maximum forward flow is determined by Newton's second law of motion for the blood column flowing into the right ventricle, C_p, and can be approximated as

$$f_{max} \approx 0.41\sigma\sqrt{\frac{A}{\rho L}\left(\frac{1}{C_v}+\frac{1}{C_p}\right)}, \qquad (3)$$

Equation (3) implies a definite scaling rule for the optimal compression frequency as a function of body weight. The ratio A/L of the dimensions of the venous blood column scales in proportion to the linear dimension of the animal or $W^{1/3}$, which is the cube root of body weight. The compliance is directly proportional to body weight, W. Hence, the argument of the square root in (3) is proportional to $W^{-2/3}$. This means that f_{max} is proportional to $W^{-1/3}$. For this algebraic model of pump filling the frequency for maximum flow, f_{max} , scales inversely with the cube root of body weight. Using expression (2) for body weight, W, compared to a theoretical 70 kg adult

$$f_{max}(W) = f_{max}(70)\left(\frac{W}{70}\right)^{-1/3} . \qquad (4)$$

Compared to adults, smaller babies or children should have a distinctly higher maximally effective compression frequency, according to a simple pump-filling model based on Newton's second law.

Estimating the numerical values of venous compliances C_v and C_p in expression (3) for a normal adult human is relatively straightforward using textbook knowledge of physiology[12]. However, the pressure vs. volume curves for veins are highly non-linear. Hence the dynamic compliances, dV/dP, of both the vena cavae and the right ventricle depend strongly on their degree of distension with blood[13, 14]. During cardiac arrest (a most extreme form of acute congestive heart failure) venous volume increases and venous compliance decreases to a value about one half normal. As shown in Online Supplement 2, reasonable estimates for venous compliances in a 70 kg adult during conditions of cardiac arrest and CPR are C_v = 11.5 ml/mmHg and and C_p = 9.0 ml/mmHg. Using these values, together with blood density 1 g/ml, A = 7 cm^2, L = 30 cm, filling time equal 1/3rd of cycle time, and 1 mmHg = 1333 g/(cm-sec^2), we can obtain the predicted compression rates for maximal blood flow given in Table 1.

The simple pump-filling hypothesis suggests that CPR compression rates should be distinctly higher for small infants than for large adults, not unlike the known differences in natural heart rates. The pump-filling model also suggests lower optimal compression rates for adults, compared to current guidelines. Values in Table 1 for subjects in the weight range of neonates or premature infants are substantially greater than 120/min, suggesting potential room for improvement, provided that humans or mechanical devices can sustain the higher rates for an adequate period of time.

To explore the scaling of optimal frequencies for chest compression with body weight in greater detail, we exercised computational models of the whole circulation, including both arterial and venous compliances, resistances of capillary beds, and inertia of blood columns in the aorta and venae cavae.

3. Computer models

For the present study we adapted the computational model shown in Figure 2 and published previously for resuscitation research by one of us[15], to include appropriate scaling of cardiovascular parameters with body size and also the effects of blood inertia in the aorta and vena cava, as described in Online Supplement 3. To simulate the redistribution of blood volume from arteries to veins during cardiac arrest and CPR, leading to increased arterial compliance and reduced venous compliance, we corrected standard normal values using the method of Online Supplement 2, so that aortic compliances for CPR are twice the values determined at normal arterial pressure and venous compliances are half the values determined at normal venous pressure. Vascular resistances in cardiac arrest may be either increased owing to endogenous epinephrine release or decreased, owing to effects of hypoxia, acidosis, and vascular collapse. Hence, we used the normal values of resistance in the computational model to explore the effects of compression rate and body size.

3.1. Cardiac and thoracic pump mechanisms

In our computational model the cardiac ventricles experience varying external pressure P_{chest} as a result of chest compression. The right atrium and thoracic aorta experience external driving pressure $f_{tp} \cdot P_{chest}$ for thoracic pump factor $0 \le f_{tp} \le 1$, depending on the degree to which the "thoracic pump" mechanism of CPR is working. In this way one can create a continuum of hybrid pump mechanisms ranging from pure cardiac pump ($f_{tp} = 0$) to pure thoracic pump ($f_{tp} = 1$), as described in reference[11]. When $f_{tp} = 1$ all mediastinal structures, including the great veins and thoracic aorta, experience a uniform "global" intrathoracic pressure rise, as originally conceived by Weisfeldt, Rudikoff and coworkers[16]. When $f_{tp} = 0$, only the right and left ventricles are pressurized, as in open chest CPR[17-19]. Intermediate values of the thoracic pump factor allow models approximating the consensus understanding[20-22], in which both mechanisms are operative to some degree. In the present study we explored effects of body size and weight over a range of thoracic pump factors.

4. Results

Figure 3 shows results of simulations of CPR in the 7 compartment circulatory model for subjects of different body weight, using vascular compliance values appropriate for cardiac arrest and CPR. The quality of CPR is represented on each vertical axis in terms of systemic perfusion pressure. Systemic perfusion pressure, defined here as mean thoracic aortic pressure minus mean right atrial pressure, is a relatively stable predictor of resuscitation success in diverse animal models[23-27]. This figure of merit has been described by Otlewski as the most valid measure of coronary perfusion pressure[28]. Figures 3(a) through 3(c) show results for increasing thoracic pump factors. In all cases flow rises as a

function of frequency to shoulder regions, and there is often a subtle peak in systemic perfusion as a function of compression frequency. The peaks are located at compression rates near 60, 120, 180, and 250 per minute for subjects weighing 70, 10, 3, and 1 kg, respectively. The peaks are more prominent when the thoracic pump factor is larger. These results are similar to those found previously in an analog model of the circulation during CPR including blood inertia[29]. Such peaks suggest that rate effects are explained in large part by tradeoffs between compression frequency and the filling time for the chest pump, related to the inertia of blood columns in the vena cava (Online Supplement 1).

As validation of the computational model of Figures 2 and 3 we compared its predictions, with the experimental results of Fitzgerald and coworkers[10], who conducted a systematic study of compression rates varying from 20 to 150 per minute in anesthetized 10 kg dogs undergoing experimental CPR with a mechanical chest compressor (Thumper®). The comparison in Figure 4 for 10 kg subjects shows that the present scaling model fits experimental data reasonably well.

5. Discussion

Given the unusual practical difficulties of working with human or animal models of cardiac arrest and CPR, theoretical and computer models have found a niche in resuscitation research[2, 30]. Such models are independent of many confounding factors present in laboratory studies and in clinical trials. These include varying patient populations, cardiac arrest time, drug therapy, underlying disease, chest configuration, and body size, as well as varying rescuer size, skill, strength, consistency, prior training, and bias. In studies of multiple compression frequencies mathematical models avoid problems caused by progressive breakdown of the chest wall, depletion of endogenous hormones, and pulmonary contusion or liver laceration with repeated trials. Mathematical models also allow exact control of the dominant hemodynamic mechanism of CPR (thoracic pump vs. cardiac pump[11, 31]).

With this approach, we found a clear effect of body size and weight on the optimal compression frequencies for CPR. The existence of plateaus and subtle peaks in the spectrum of systemic perfusion pressures versus frequency and their relative separation in the compression frequency domain are explained in part by tradeoffs between compression frequency and pump filling time (Online Supplement 1). The overall amplitude of systemic perfusion pressure is strongly modulated by thoracic pump factor. The locations of the peaks in perfusion pressure along the frequency axis, however, are relatively independent of the thoracic pump factor but strongly dependent upon body size.

Our study is limited in that it uses simplified models of the circulation that do not reflect specific underlying disease states. We do not specifically model pre-existing congestive heart failure, which could decrease venous compliance by means of venous distension and in turn increase the optimal compression frequency. We also do not specifically model hemorrhage, which could have the opposite effect. We ignore increases in peripheral

vascular resistance caused by endogenous or exogenous vasoconstrictors as well as decreases caused by hypoxia and acidosis.

The analytical model of pump-filling described in Online Supplement 1 does not account for the closed loop nature of an intact circulation, in which, if pump filling is poor on one beat at high compression rates, venous pressure increases transiently and there is more filling on the next beat. This alternans-like phenomenon is quite evident in pressure read-outs from the closed loop computational model at high compression frequencies. The effect supports perfusion at higher compression rates to a degree greater than that predicted by the simple pump-filling model summarized in Equation (3). However, the predictions of Equation (3) regarding of the existence of peaks in perfusion and their locations in the frequency domain have been confirmed by more complex models (Figure 3) and by experiment (Figure 4).

6. Conclusions

There may be merit in exploring substantially slower compression frequencies for CPR in the world of adult medicine. Compression frequencies near 60/min (the original 1960 guideline recommendation) may be less tiring for rescuers and less traumatic for the patient than higher compression rates. Slower compressions would allow for better pump filling and also more complete chest recoil, as well as more attention to the optimal "rectangular shape" of the compression waveform[32], which is quite difficult to achieve at higher frequencies. Slower compressions in adults may even be of psychological benefit to the resuscitation team, being less frenetic and hurried.

In smaller patients, especially infants and neonates, there are fundamental physical and mathematical reasons why improved blood flow may results from compression rates substantially faster than those effective in adult patients. These include the effects of the mass of venous blood columns entering the chest pump as described by Newton's second law of motion and the way in which mass, length, and area scale with body size.

In adult humans there may be some room for improvement at the bottom of the compression frequency scale. In neonates there is room for improvement at the top.

References

1. Babbs CF. Interposed abdominal compression CPR: a comprehensive evidence based review. Resuscitation 2003; 59:71-82.
2. Babbs CF. Circulatory adjuncts. Newer methods of cardiopulmonary resuscitation. Cardiol Clin 2002; 20:37-59.
3. Guidelines 2000 for cardiopulmonary resuscitation and emergency cardiovascular care: international consensus on science. Circulation 2000; 102 (suppl I):I-1--I-384.
4. Dean JM, Koehler RC, Schleien CL, et al. Age-related effects of compression rate and duration in cardiopulmonary resuscitation. J Appl Physiol 1990; 68:554-60.
5. Dean JM, Koehler RC, Schleien CL, et al. Improved blood flow during prolonged cardiopulmonary resuscitation with 30% duty cycle in infant pigs. Circulation 1991; 84:896-904.
6. 2005 American Heart Association (AHA) guidelines for cardiopulmonary resuscitation (CPR) and emergency cardiovascular care (ECC) of pediatric and neonatal patients: pediatric basic life support. Pediatrics 2006; 117:e989-1004.
7. Schmidt-Nielsen K. Scaling: Why is animal size so important? Cambridge: Cambridge University Press, 1984.
8. Honig CR. Modern Cardiovascular Physiology. Boston: Little, Brown and Company, 1981:374.
9. Posey J, Geddes L. Measurement of the modulus of elasticity of the arterial wall. Cardiovascular Research Center Bulletin 1973; 11:83-103.
10. Fitzgerald KR, Babbs CF, Frissora HA, Davis RW, Silver DI. Cardiac output during cardiopulmonary resuscitation at various compression rates and durations. American Journal of Physiology 1981; 241:H442-H448.
11. Babbs CF. New versus old theories of blood flow during cardiopulmonary resuscitation. Critical Care Medicine 1980; 8:191-195.
12. Boron WF, Boulpaep EL. Medical Physiology. Philadelphia: Elsevier, 2005:1319.
13. Fung YC. Biomechanics: mechanical properties of living tissues. New York: Springer-Verlag, 1981.
14. Fung YC. Biomechanics: Circulation. New York: Springer-Verlag, 1997:571 pages.
15. Babbs CF. CPR techniques that combine chest and abdominal compression and decompression: Hemodynamic insights from a spreadsheet model. Circulation 1999; 100:2146-2152.
16. Rudikoff MT, Maughan WL, Effron M, Freund P, Weisfeldt ML. Mechanisms of blood flow during cardiopulmonary resuscitation. Circulation 1980; 61:345-352.
17. Weiser FM, Adler LN, Kuhn LA. Hemodynamic effects of closed and open chest cardiac resuscitation in normal dogs and those with acute myocardial infarction, Am J Cardiol, 1962. Vol. 10.
18. Sanders AB, Kern KB, Ewy GA, Atlas M, Bailey L. Improved resuscitation from cardiac arrest with open chest massage, Annal Emerg Med 13, 1984.
19. Babbs CF. Hemodynamic mechanisms in CPR: a theoretical rationale for resuscitative thoracotomy in non-traumatic cardiac arrest. Resuscitation 1987; 15:37-50.

20. Paradis NA, Martin GB, Goetting MG, et al. Simultaneous aortic, jugular bulb, and right atrial pressures during cardiopulmonary resuscitation in humans: Insights into mechanisms. Circulation 1989; 80:361-8.
21. Halperin HR, Tsitlik JE, Guerci AD, et al. Determinants of blood flow to vital organs during cardiopulmonary resuscitation in dogs. Circulation 1986; 73:539-50.
22. Chandra NC. Mechanisms of blood flow during CPR. Ann Emerg Med 1993; 22:281-8.
23. Pearson JW, Redding JS. Influence of peripheral vascular tone on cardiac resuscitation. Anesth Analg 1965; 44:746-752.
24. Redding JS. Abdominal compression in cardiopulmonary resuscitation. Anesthesia and Analgesia 1971; 50:668-675.
25. Ralston SH, Voorhees WD, Babbs CF. Intrapulmonary epinephrine during cardiopulmonary resuscitation: Improved regional blood flow and resuscitation in dogs. Annals of Emergency Medicine 1984; 13:79-86.
26. Ralston SH, Showen L, Carter A, Tacker WA. Comparison of endotracheal and intravenous epinephrine dosage during CPR in dogs. Annals of Emergency Medicine 1985; 14:494-495.
27. Kern KB, Ewy GA, Voorhees WD, Babbs CF, Tacker WA. Myocardial perfusion pressure: a predictor of 24-hour survival during prolonged cardiac arrest in dogs. Resuscitation 1988; 16:241-250.
28. Otlewski M. The use of six types of CPR to determine whether published methods of calculating coronary perfusion pressure produce differing results. Basic Medical Sciences, Purdue University. West Lafayette, Indiana, 2007.
29. Babbs CF, Weaver JC, Ralston SH, Geddes LA. Cardiac, thoracic, and abdominal pump mechanisms in CPR: studies in an electrical model of the circulation. American Journal of Emergency Medicine 1984; 2:299-308.
30. Christenson JM. Cardiopulmonary resuscitation research models: motherboards, mammals, and man. Acad Emerg Med 1995; 2:669-71.
31. Babbs CF, Weaver JC, Ralston SH, Geddes LA. Cardiac, thoracic, and abdominal pump mechanisms in cardiopulmonary resuscitation: studies in an electrical model of the circulation. Am J Emerg Med 1984; 2:299-308.
32. Jung E, Lenhart S, Protopopescu V, Babbs CF. Optimal control theory applied to a difference equation model for cardiopulmonary resuscitation. Mathematical Models and Methods in Applied Sciences 2005; 15:1519-1531.

Table

Table 1. Compression frequencies, f_{max}, for maximal blood flow according to a simple biomechanical model of chest pump filling, including blood inertia, which is described in detail in the Online Supplement 1.

Lean body weight, W (kg)	$(W/70)^{0.333}$	f_{max} (1/min)
70	1.00	64
20	0.65	99
10	0.52	124
5	0.41	157
3	0.35	184
2	0.30	214
1	0.24	267

Figures

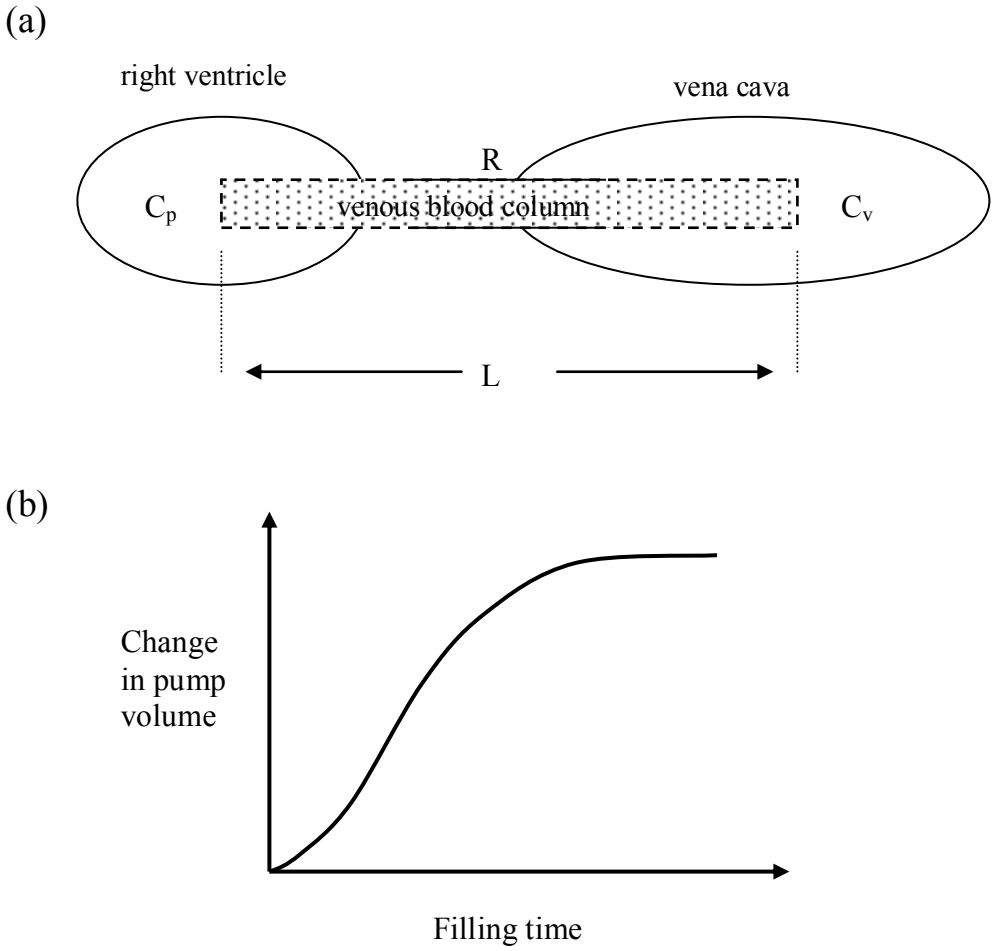

Figure 1. (a) Two-compartment model of the great veins C_v (right) and chest pump C_p (left) during filling, connected by low resistance R of the open tricuspid valve. (b) Sketch of sigmoid pump volume increase as a function of time during filling.

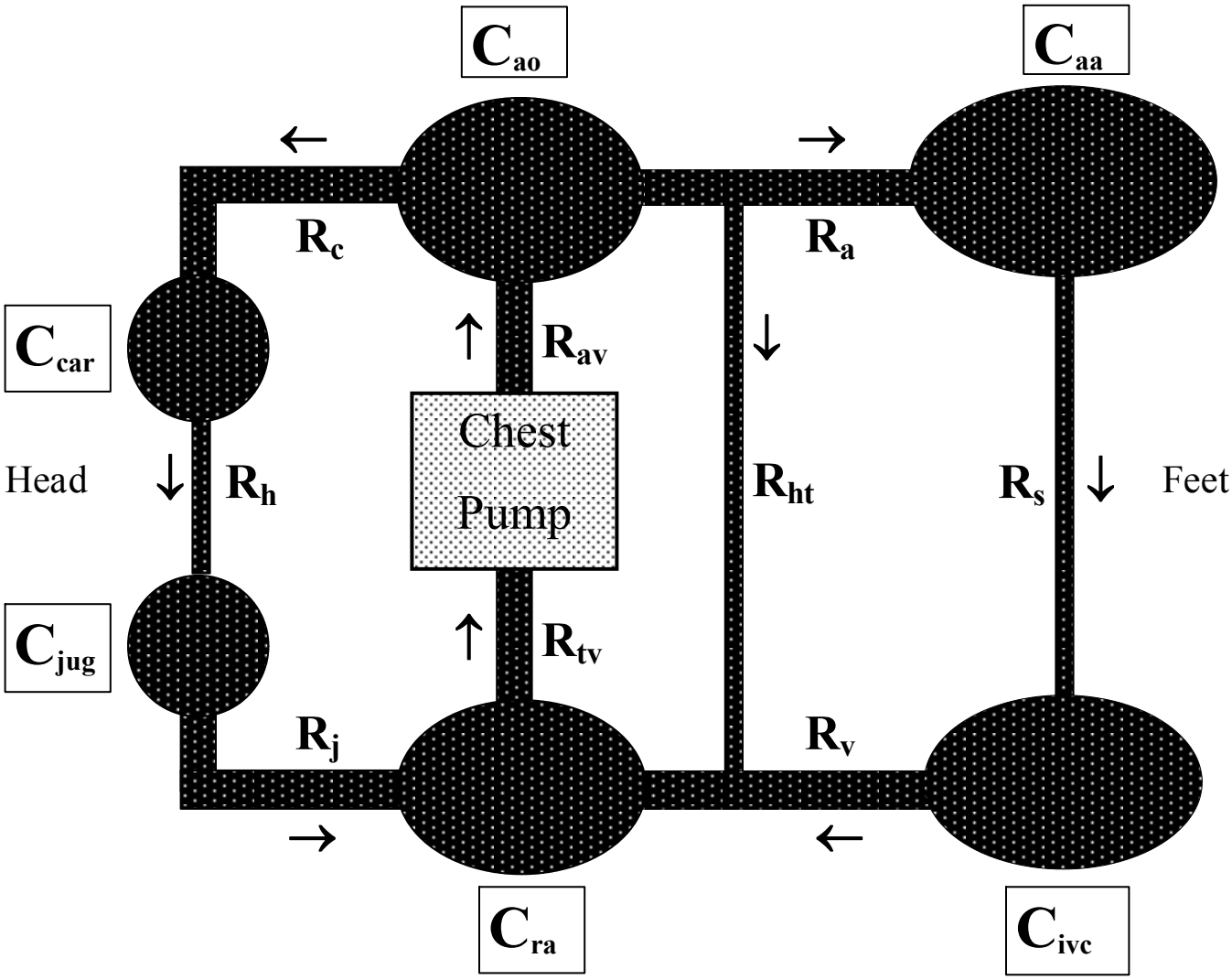

Figure 2. Seven compartment model of the human circulatory system. Definitions of compliances, C, resistances, R, are as follows: carotid arteries (car), thoracic aorta (ao), abdominal aorta (aa), inferior vena cava (ivc), jugular veins (jug), right atrium (ra), and chest pump mechanism. Non-zero vascular resistances, R, connect the vascular compartments. The value of R_{ht} is large and represents the vascular resistance of the heart and miscellaneous tissues within chest. The value of R_s is intermediate and represents the vascular resistance of all tissue beds outside the chest, including arms, legs, and abdomen. The values of R_a, and R_v, are small and represent lumped in-line resistances of the great vessels between the chest and the abdomen, as are the values of R_c and R_j leading to the head and neck. The remaining small resistances represent outflow and inflow resistances of the cardiac valves, denoted by suitable anatomic subscripts.

(a)

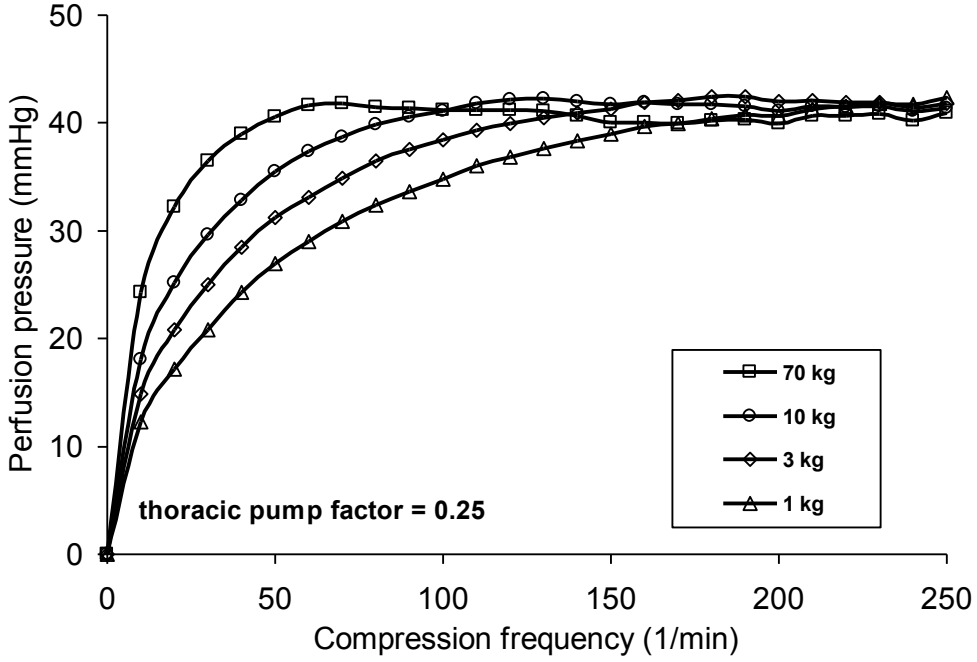
Perfusion pressure (mmHg)
Compression frequency (1/min)
thoracic pump factor = 0.25
70 kg
10 kg
3 kg
1 kg
0
10
20
30
40
50
0
50
100
150
200
250

(b)

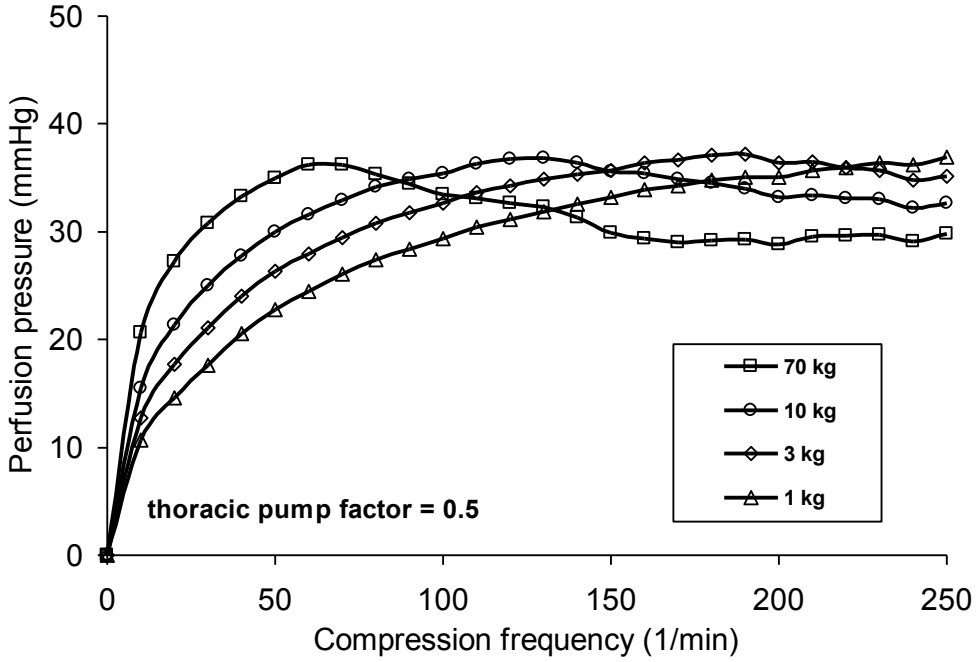
Perfusion pressure (mmHg)
Compression frequency (1/min)
thoracic pump factor = 0.5
70 kg
10 kg
3 kg
1 kg
0
10
20
30
40
50
0
50
100
150
200
250

(c)

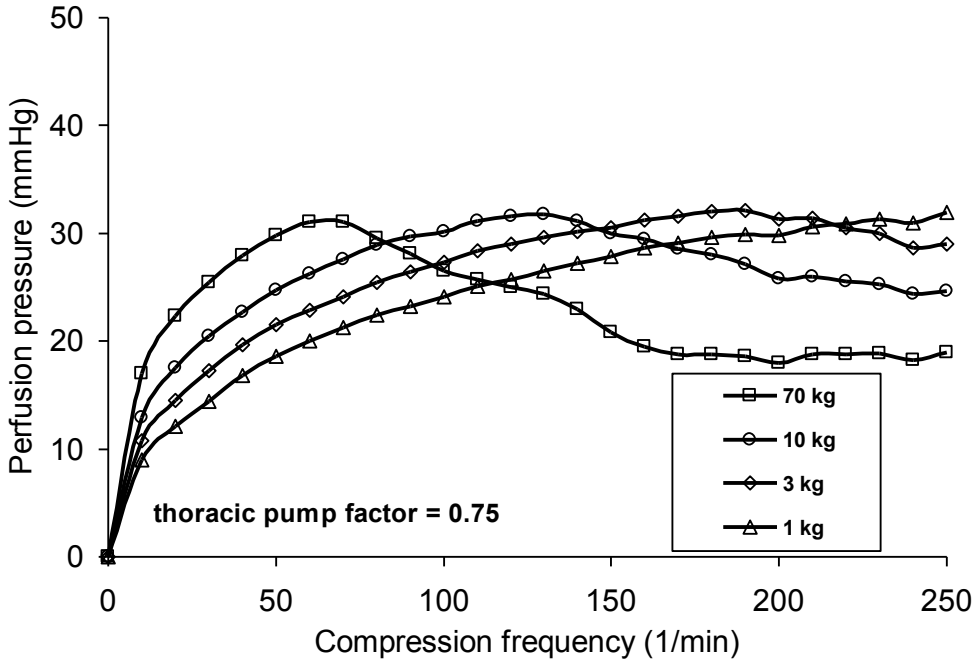

Figure 3. Cardiopulmonary pressures in simulations of CPR for subjects of different body weight. Systemic perfusion pressure (mean thoracic aortic minus mean central venous pressure) is plotted as a function of chest compression frequency. Blood density is 1.05 g/ml. Thoracic pump factors are (a) 0.25, (b) 0.50, and (c) 0.75.

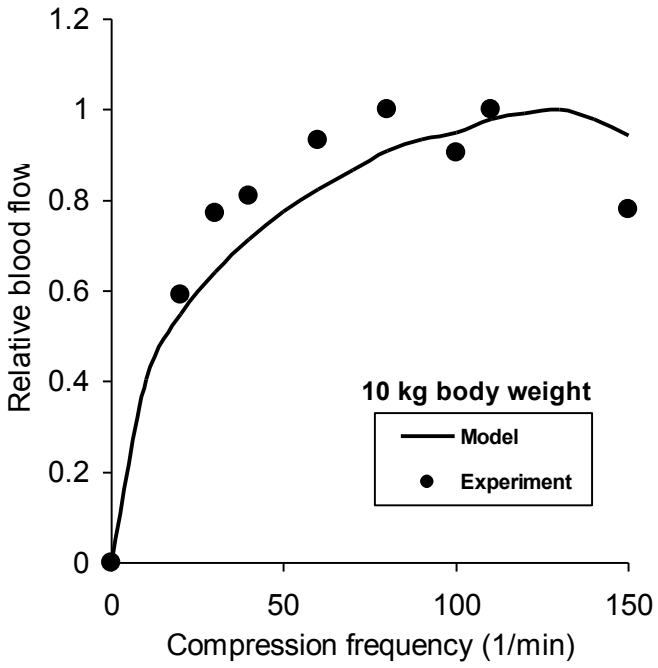

Figure 4. Computational model vs. experimental data from Fitzgerald et al. (1981). The fraction of maximal blood flow is plotted as a function of chest compression frequency. Thoracic pump factor for model calculations is 0.75. Corresponding curves (not shown) for thoracic pump factors of 0.25, 0.5, and 1.00 are very similar. Data points are means of experimental results.

Online Supplement 1: pump filling hypothesis including blood inertia

To describe filling-related tradeoffs quantitatively, imagine an exceedingly simple two compartment model shown in Figure 1 in which the elastic central venous reservoir (lumped venae cavae and right atrium at the right of the diagram) is connected to the input reservoir (right ventricle) of an elastic chest pump on the left by a low resistance pathway that includes the tricuspid valve. The valve prevents backflow when the pump is compressed externally, and we are interested in the fluid inflow, i , that occurs after valve opening during decompression of the pump. The elastic venous reservoir and the elastic pumping chamber are characterized by compliances C_v and C_p .

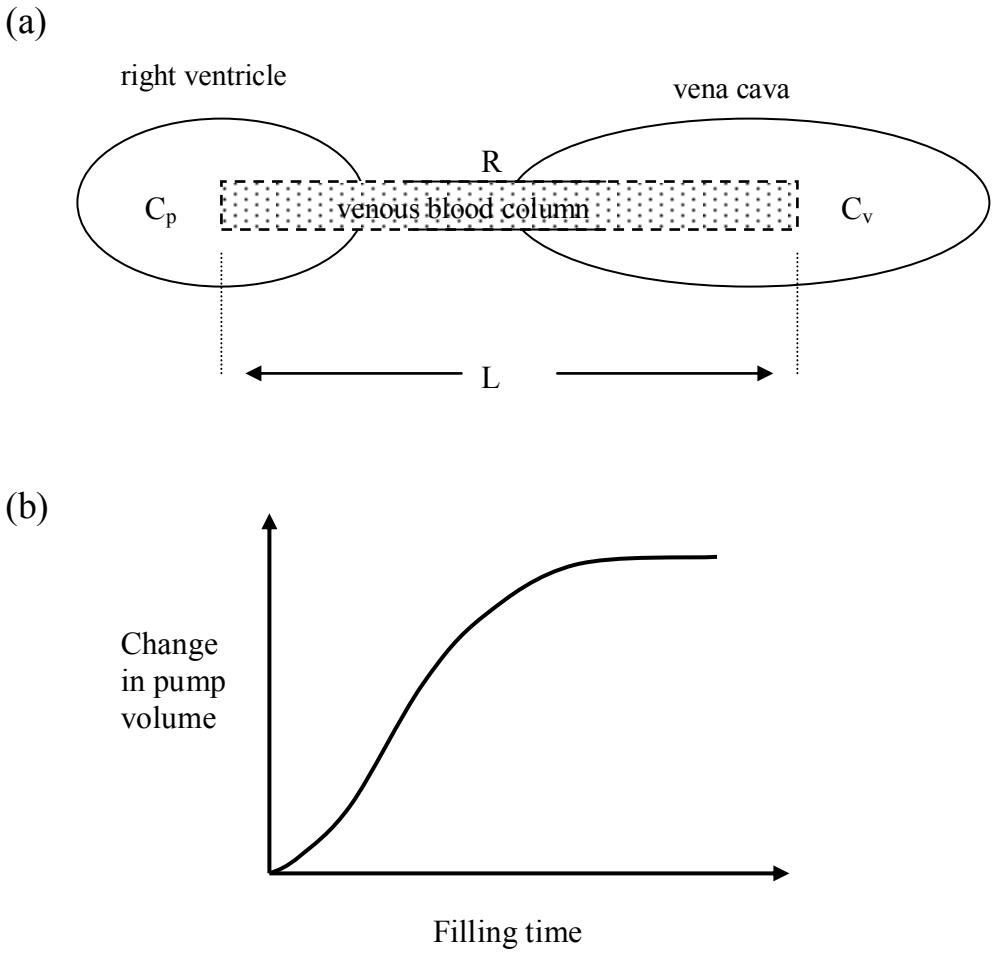

Figure 1. (a) Two-compartment model of the great veins C_v (right) and chest pump C_p (left) during filling, connected by low resistance R of the open tricuspid valve. (b) Sketch of sigmoid pump volume increase as a function of time during filling.

Consider Newton's second law (force = mass × acceleration or F = ma) to describe, as a first step, the motion of the venous blood column with nonzero mass as it flows into the right ventricle (C_p) with negligible resistance, under the influence of axial pressure difference, ΔP, between the two vascular compartments. For simplicity assume that the cross sectional area, A, and length, L, are constant, and the mass density of blood is ρ. As can be shown by more complex analysis, is reasonable to ignore the small resistance of the tricuspid valve and vena cava, which has a trivial influence on the results. Then

$$F = ma = \rho LA \cdot \frac{d}{dt}\left(\frac{i}{A}\right) = A \cdot \Delta P, \text{ and by differentiation } \frac{d(\Delta P)}{dt} = \frac{\rho L}{A}\frac{d^2 i}{dt^2} \qquad (1)$$

Now consider sources of the pressure difference in terms of compliances of the time rate of change of ΔP in terms of axial flow, i , from the vena cava, C_v to the right ventricle C_p. For simplicity, suppose that during the brief time of pump opening in mid to late decompression the chest pressure has diminished to a roughly a steady level, so the rate of change in chest pressure can be ignored. Then for compartmental volumes, V,

$$\frac{d(\Delta P)}{dt} = \frac{1}{C_v}\frac{dV_v}{dt} - \frac{1}{C_p}\frac{dV_p}{dt} = -\frac{1}{C_v}i - \frac{1}{C_p}i = -\left(\frac{1}{C_v} + \frac{1}{C_p}\right)i. \qquad (2)$$

Equating (1) and (2) we have a simple second order differential equation for pump filling rate, i(t) in cm^3 of blood per second, as a function of time, t.

$$\frac{\rho L}{A}\frac{d^2 i}{dt^2} + \left(\frac{1}{C_v} + \frac{1}{C_p}\right)i = 0 \qquad (3)$$

The relevant solution to differential equation (3) is that inflow, $i = a \cdot \sin(\omega t)$, for constant, a , related to the depth of chest compression, and angular frequency, ω, describing the resonant physical properties of the system. Integrating (3) and using the method of undetermined coefficients it is straightforward to deduce that

$$\omega = \sqrt{\frac{A}{\rho L}\left(\frac{1}{C_v} + \frac{1}{C_p}\right)}\ . \qquad (4)$$

More importantly, the pump volume $V_p(t)$ for filling time, t , after tricuspid valve opening can be written as

$$V(t) = \int_0^t i(t)dt = \frac{a}{\omega}\left(1 - \cos(\omega t)\right). \qquad (5)$$

The function (5) is a sigmoid curve with maximal filling at $\omega t = \pi$ radians or time $t = \pi/\omega$. For longer cycle times (i.e. slower compression frequencies) filling is complete,

and the tricuspid valve prevents backflow. Hence $V_{max} = 2a/\omega$, or $a = \omega V_{max}/2$. Thus the filling volume, which is the stroke volume of the chest pump, is

$$V(t) = \frac{V_{max}}{2}\left(1 - \cos(\omega t)\right) \quad \text{for } 0 \le t \le \pi/\omega, \text{ and}$$

$$V(t) = V_{max} \qquad \text{for } t > \pi/\omega. \tag{6}$$

As t ranges from zero to π/ω, the $\cos(\omega t)$ ranges from 1 to –1, and V(t) ranges from zero to V_{max}. For smaller filling times at higher compression frequencies, stroke volume is limited.

Forward blood flow or "cardiac output" in CPR is the product of compression rate and stroke volume. Let f indicate the frequency of chest compression in units of either Hz or compressions per minute. Suppose that pump filling occurs during a particular fraction, σ, of the cycle time, such as 1/3. In this case filling time, $t = \sigma/f$. Forward flow is compression rate × stroke volume, or

$$\text{Flow} = f V_{max} \quad \text{for } f \le \sigma\omega/\pi$$

at lower frequencies when complete filling occurs, and

$$\text{Flow} = f\,\frac{V_{max}}{2}\left(1 - \cos(\omega\sigma / f)\right) \quad \text{for } f > \sigma\omega/\pi \tag{7}$$

at higher frequencies when partial filling occurs.

Thus, according to this simple conceptual model, blood flow is zero at zero compression frequency and increases linearly as a function of frequency as long as there is time for complete filling. Then, as frequency continues to increase, flow diminishes. The shoulder of the roll-off in flow begins when frequency $f_1 = \sigma\omega/\pi$, or $f_1 \approx 0.32\,\sigma\omega$. Flow continues toward a maximum value when the derivative $\frac{d}{df}(\text{Flow}) = 0$, which can be shown either by calculus (substituting series expansions for the sine and cosine functions), as shown in the Appendix to this supplement, or by trial-and-error, to occur when the chest compression frequency is

$$f_{max} \approx \frac{\sigma\omega}{\sqrt{\pi^2 - 4}} = 0.41\sigma\omega, \text{ or} \tag{8a}$$

$$f_{max} \approx 0.41\sigma\sqrt{\frac{A}{\rho L}\left(\frac{1}{C_v} + \frac{1}{C_{pump}}\right)}, \tag{8b}$$

where, as expected, f_{max} is somewhat greater than $f_1 = \sigma\omega/\pi = 0.32\sigma\omega$ at the end of the linear ramp of flow vs. compression frequency.

Appendix to Supplement 1

The flow vs. frequency function is

$$\text{Flow} = f\,\frac{V_{max}}{2}\left(1-\cos(\omega\sigma/f)\right).$$

The series approximation of the cosine for "small" deviations of x from π is $\cos(\pi+x) \approx -(1 - x^2/2)$. For = $\sigma\omega/f$ close to π, as expected, we can use the series approximation to simplify the calculus by substituting

$$\cos\left(\frac{\sigma\omega}{f}\right) \approx \frac{1}{2}\left(\frac{\sigma\omega}{f}-\pi\right)^2 - 1$$

so that

$$\text{Flow} \approx f\,\frac{V_{max}}{2}\left(2-\frac{1}{2}\left(\frac{\sigma\omega}{f}-\pi\right)^2\right) \text{ or}$$

$$\text{Flow} \approx V_{max}\left(f-\frac{1}{4}\left(\frac{\sigma^2\omega^2}{f}-2\sigma\omega\pi+f\,\pi^2\right)\right).$$

To find the maximum using calculus set d(Flow)/df = 0:

$$0 \approx \left(1-\frac{1}{4}\left(-\frac{\sigma^2\omega^2}{f^2}+\pi^2\right)\right) \quad \text{or} \quad \pi^2-4 \approx \frac{\sigma^2\omega^2}{f^2},$$

which leads to

$$f \approx \frac{\sigma\omega}{\sqrt{\pi^2-4}} = 0.41\sigma\omega.$$

Online Supplement 2: treatment of nonlinear vascular compliances in CPR

Nonlinear model of vessel compliance

During cardiac arrest blood drains from arteries to veins, as arterial pressure drops toward zero. There is profound venous pooling. The heart is not pumping blood out of the veins in cardiac arrest, so it remains in veins. This overload makes the veins stiffer. Because venous compliance is highly non-linear, the stretched veins in cardiac arrest could be significantly less compliant than under normal conditions used reflected in the calculations of normal venous compliance for both adults and neonates.

A simple and powerful nonlinear model for finding the dynamic compliance of a tube made of a classical Fungian biomaterial, (Y. C. Fung, Biomechanics: mechanical properties of living tissues, Springer-Verlag, New York, 1981) takes the form

$$P = P_0\left(e^{b(v-v_0)/v_0}\right). \tag{1}$$

Here P is the transmural distending pressure for the vessel. The reference pressure P_0 refers to the pressure at which a fixed experimental value for dynamic compliance, C_0, is determined, such as normal distending pressure.

To get nonlinear dynamic compliance, we can recast (1) as,

$$\ln\left(\frac{P}{P_0}\right) = \frac{b(V-V_0)}{V_0}, \quad \text{or} \quad V = V_0 + \frac{V_0}{b}\cdot\ln\left(\frac{P}{P_0}\right). \tag{2}$$

The dynamic compliance is by definition

$$\frac{dV}{dP} = \frac{V_0}{b}\cdot\frac{1}{\frac{P}{P_0}}\cdot\frac{1}{P_0} = \frac{V_0}{b}\cdot\frac{1}{P}.$$

When $P = P_0$ we have $\frac{dV}{dP} = \frac{V_0}{b}\cdot\frac{1}{P_0} = C_0$, and so $\frac{V_0}{b} = C_0 P_0$. Therefore

$$\frac{dV}{dP} = C_0\cdot\frac{P_0}{P} \tag{3}$$

as a function of pressure only.

Thus we can convert normal compliances, C_0, to nonlinear, pressure dependent ones, using (3). In CPR arterial pressures fall from a mean near 95 mmHg to a mean near 40 mmHg. Central venous and right ventricular filling pressures increase from a mean near 5

mmHg to a mean near 10 mmHg. Thus reasonable estimates for arterial compliances in CPR, given non-linear vascular compliances, are twice normal values for the aorta and half normal values for the vena cava and right heart.

Evaluation of constants

Based on the following observations from normal adult physiology and anatomy (box below), one can find numerical estimates for normal adult values of constants C_v, C_p, and $\rho L/A$. To estimate compliances from normal pressure and volume data consider the pressure changes that accompany normal physiological volume changes. In computing the net volume change in the vena cavae during right ventricular filling, one should recognize that venous return continues while the ventricles are filling at a rate approximately equal to the cardiac output.

Summary of relevant physiology in a normal adult

Blood density is about that of water, the diameter of the adult vena cava is about 3 cm, and the combined lengths of the superior and inferior venous blood columns entering the right atrium total about 30 cm. The normal stroke volume is about 70 ml/beat. When the tricuspid valve opens and blood quickly enters the right ventricle during rapid ventricular filling, the central venous (caval) pressure falls about 2 mmHg (the so-called y-descent of the jugular venous pulse). At the same time the pressure in the right ventricle increases about 4 mmHg. The normal heart rate is 80/min, and ventricular filling happens during about 1/3rd of the cycle time. Also 1 mmHg = 1333 g/(cm-sec^2).

Using the forgoing benchmark normal data we can deduce the following.

$\rho = 1\ g/cm^3$

$A = \pi(1.5\ cm)^2 = 7.0\ cm^2$

$L = 30\ cm$

During right ventricular filling the stroke volume is going into right ventricle, but cardiac output is returning blood to the veins during 1/3 of the cardiac cycle. If venous return is steady, then a net 2/3 of the stroke volume leaves the great veins during ventricular filling or about 47 ml. In this case

$$C_v = \frac{-47 cm^3}{-2 mmHg} = 23 \frac{cm^3}{mmHg}$$

$C_p = 70\ cm^3/4\ mmHg = 18\ cm^3/mmHg$

$\rho L/A = 1\times 30/7 = 4.3\ \mathrm{g/cm^4}$

$$\frac{1}{C_v}+\frac{1}{C_p}=0.099\frac{\mathrm{mmHg}}{\mathrm{cm^3}}\frac{1333\mathrm{g}}{\mathrm{mmHg}}\frac{1}{\mathrm{cm}\cdot\mathrm{sec^2}}=132\frac{\mathrm{g}}{\mathrm{cm^4}\cdot\mathrm{sec^2}}$$

The forgoing estimates are based on the normal adult values. During venous distension in cardiac arrest, however, we estimate that mean arterial pressure is about half that prevailing during the normal circulation and distending venous pressure is about twice the normal central venous pressure. In this case for the pump-filling model, we would have

$$\frac{1}{C_v}+\frac{1}{C_p}=2\cdot 132\frac{\mathrm{g}}{\mathrm{cm^4}\cdot\mathrm{sec^2}}=264\frac{\mathrm{g}}{\mathrm{cm^4}\cdot\mathrm{sec^2}},$$

$$\text{so }\sqrt{\frac{A}{\rho L}\left(\frac{1}{C_v}+\frac{1}{C_p}\right)}=\sqrt{\frac{264}{4.3}}=7.8\frac{1}{\mathrm{sec}}.$$

In this case the optimal frequency for chest compression in adult CPR is

$$f_{max}\approx 0.41\sigma\sqrt{\frac{A}{\rho L}\left(\frac{1}{C_v}+\frac{1}{C_p}\right)}=0.41\cdot\frac{1}{3}\cdot 7.8\frac{1}{\mathrm{sec}}\cdot\frac{60\mathrm{sec}}{\mathrm{min}}=64/\mathrm{min}.$$

Online Supplement 3: computer models

For the present study we adapted the computational model shown in text Figure 2, reproduced below, and include appropriate scaling of cardiovascular parameters with body size and the effects of blood inertia in the aorta and vena cava. The model includes seven compliant chambers, connected by resistances through which blood may flow, to represent the human circulatory system. Definitions of model components are given in Table S3.1 below.

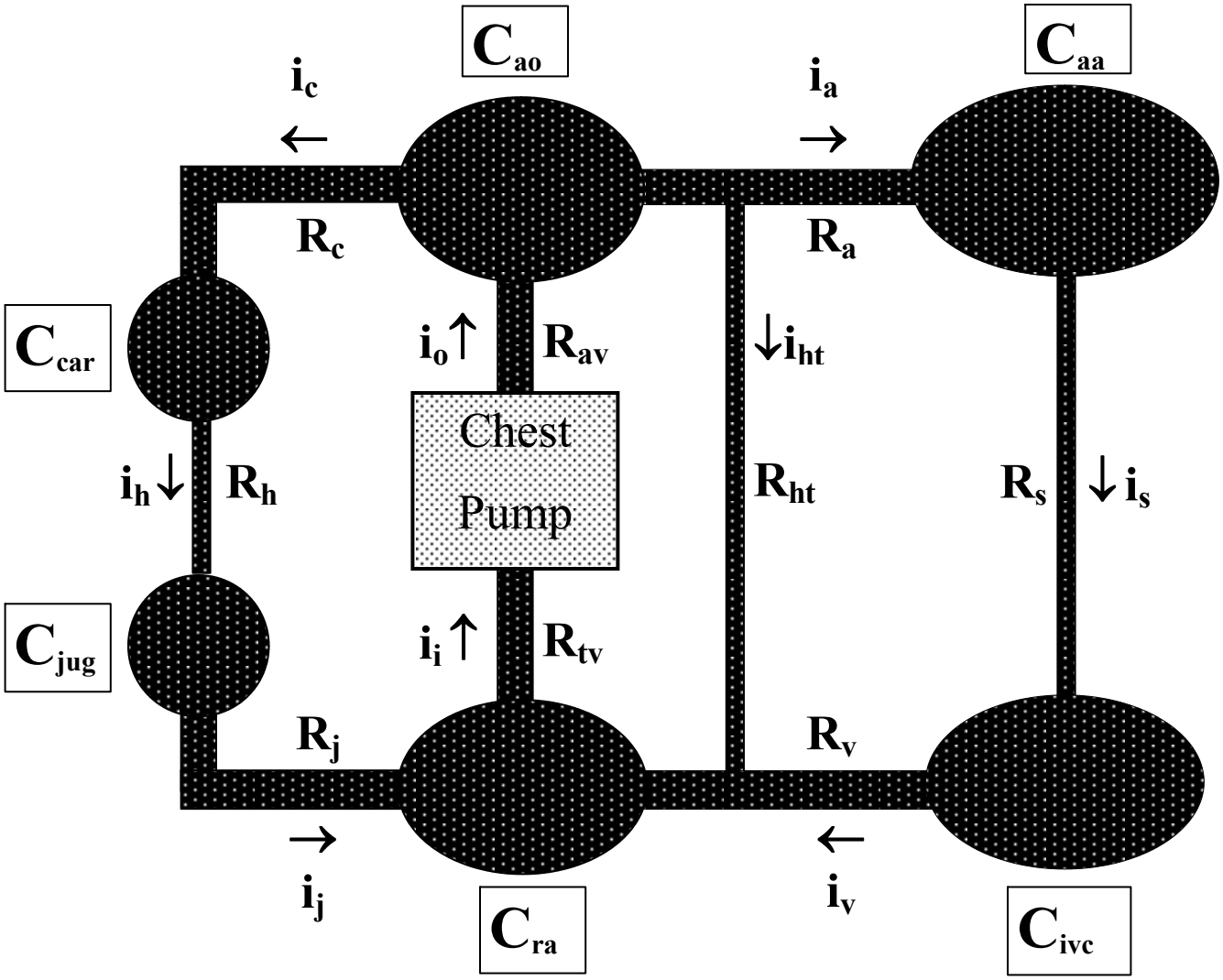

Text Figure 2. Seven compartment model of the human circulatory system. Here flows, i , are explicitly shown. Definitions of variables are provided in Table S3.1

Table S3.1. Components of a simple model of the circulatory system

Resistances	**Compliances**
R_c , R_j carotid arteries and jugular veins	C_{ao} thoracic aorta
R_a, R_v , small in-line resistances of the aorta and the vena cava	C_{aa} abdominal aorta, carotids, and other large arteries
R_s systemic body tissues in abdomen, arms, legs	C_{ivc} inferior vena cava, and other extrathoracic veins
R_{av} small in-line resistance of the aortic valve	C_{car} carotid arteries
R_{tv} resistance of the tricuspid valve	C_{jug} jugular veins
R_h capillaries in the head	C_{ra} right atrium and superior vena cava
R_c resistance of carotid arteries	C_{pump} chest pump
R_{ht} resistance of coronary vascular beds	

The compliances correspond to the carotid arteries (car), thoracic aorta (ao), abdominal aorta (aa), inferior vena cava (ivc), jugular veins (jug), right atrium (ra), and chest pump mechanism (pump). Non-zero vascular resistances, R, connect the vascular compartments. The value of R_{ht} is large and represents the vascular resistance of the heart and miscellaneous tissues within chest. The value of R_s is intermediate and represents the vascular resistance of all tissue beds outside the chest, including arms, legs, and abdomen. The values of R_a, and R_v, are small and represent lumped in-line resistances of the great vessels between the chest and the abdomen, as are the values or R_c and R_j leading to the head and neck. The remaining small resistances represent outflow and inflow resistances of the cardiac valves, denoted by suitable anatomic subscripts. Positive directions of blood flows between compartments of the model (arrows) are those of the normal circulation. In Figure 2 currents i_c (carotid), i_a (aortic), i_h (head), i_s (systemic), i_v (venous), i_j (jugular), i_i (pump input), and i_o (pump output) are shown for clarity, with positive directions specified by arrows. Also include are Niemann's valves between the chest and jugular veins at the level of the thoracic inlet. These are actual, but little known anatomic structures in humans* that function to block headward transmission of large positive pressure pulses in the chest during cough and also during CPR. (See Niemann JT, Ung S, Rosborough JP, Suzuki J, Criley JM. Preferential brachiocephalic flow during CPR--a hemodynamic explanation. Circulation 64(IV) 1981:303.)

* Gray's anatomy describes these valves. "The left [internal jugular] vein is generally smaller than the right, and each contains a pair of valves, which are placed about 2.5 cm. above the termination of the vessel." Henry Gray, Anatomy of the Human Body, 1918.

Computation of compartmental pressures

To compute a marching solution for pressures in the system over time, we begin with the definition of compliance for a hollow elastic blood vessel, namely $C = \Delta V/\Delta P$, for blood volume increment ΔV and blood pressure increment ΔP. The approach for a typical compartment is as follows.

$\Delta P = \frac{1}{C}\Delta V$, and in turn, taking time derivatives, $\frac{d(\Delta P)}{dt} = \frac{1}{C}\frac{d(\Delta V)}{dt} = \frac{1}{C}(i_{in} - i_{out})$,

where i_{in} is the rate of blood flow into a compartment with compliance C, and i_{out} is the rate of outflow. This expression gives the change in compartment pressure because of filling and emptying. Although blood vessel compliance is non-linear over a wide range of distending pressures, over a limited range of pressures, including diastolic to systolic arterial pressure, a single value of compliance can suffice. A similar argument can be made for normal vascular resistances, here represented as constants.

Next one can use Ohm's law to substitute for each compartmental i_{in} or i_{out} in terms of neighboring compartment pressures. For example, the inflow to the extrathoracic systemic veins through R_s would be $(P_{aa} - P_{ivc})/R_s$. In turn, for constant compliances, C, and constant resistances, R, one can generate a system of coupled differential equations for pressures, P, in the 7 compartments of the circulatory model. Keeping track of the correct positive direction of blood flow indicated by the arrows in Figure 2, the detailed equations in system (1) below are obtained. In this set of coupled differential equations for resistive flow the function max(a , b), which equals the greater of values a and b, is used to mimic the action of the cardiac valves and of Niemann's valves. The intrathoracic or mediastinal pressure, P_{chest}, caused by chest compression is described subsequently.

$$
\begin{cases}
\dfrac{dP_{pump}}{dt} = \dfrac{dP_{chest}}{dt} + \dfrac{1}{C_{pump}}\left[\dfrac{\max\left(0, P_{ra} - P_{pump}\right)}{R_{tv}} - \dfrac{\max\left(0, P_{pump} - P_{ao}\right)}{R_{av}}\right] \\
\dfrac{dP_{ao}}{dt} = \dfrac{1}{C_{ao}}\left[\dfrac{\max\left(0, P_{pump} - P_{ao}\right)}{R_{av}} - \dfrac{P_{ao} - P_{rh}}{R_{ht}} - \dfrac{P_{ao} - P_{aa}}{R_{a}} - \dfrac{P_{ao} - P_{car}}{R_{c}}\right] \\
\dfrac{dP_{aa}}{dt} = \dfrac{1}{C_{aa}}\left[\dfrac{P_{ao} - P_{aa}}{R_{a}} - \dfrac{P_{aa} - P_{ivc}}{R_{s}}\right] \\
\dfrac{dP_{ivc}}{dt} = \dfrac{1}{C_{ivc}}\left[\dfrac{P_{aa} - P_{ivc}}{R_{s}} - \dfrac{P_{ivc} - P_{ra}}{R_{v}}\right] \\
\dfrac{dP_{ra}}{dt} = \dfrac{1}{C_{ra}}\left[\dfrac{P_{ao} - P_{ra}}{R_{ht}} + \dfrac{P_{ivc} - P_{ra}}{R_{v}} + \dfrac{\max\left(0, P_{jug} - P_{ra}\right)}{R_{j}} - \dfrac{\max\left(0, P_{ra} - P_{pump}\right)}{R_{tv}}\right] \\
\dfrac{dP_{car}}{dt} = \dfrac{1}{C_{car}}\left[\dfrac{P_{ao} - P_{car}}{R_{c}} - \dfrac{P_{car} - P_{jug}}{R_{h}}\right] \\
\dfrac{dP_{jug}}{dt} = \dfrac{1}{C_{jug}}\left[\dfrac{P_{car} - P_{jug}}{R_{h}} - \dfrac{\max\left(0, P_{jug} - P_{ra}\right)}{R_{j}}\right]
\end{cases}
\tag{1}
$$

Inertance of aortic and caval blood columns

The coupled differential equations in (1) do not take into account inertia of longer columns of blood, which may be important in the timing of pump filling. To correct for inertial effects, consider the blood flow between any two elastic compartments 1 and 2 of the model having compliances C_1 and C_2, connected by a channel with resistance R filled with a blood column having inertance I (blood density times length divided by area). Based on Newton's second law of motion the corrected flow between the compartments, i' , including inertial effects, is described by

$$P_1 - P_2 = i'R + I\frac{di'}{dt}. \tag{2}$$

Here blood flow i' is considered positive if flowing in the direction from C_1 to C_2. Resistive flow between compartments, as would be computed from system (1), is

$$\frac{P_1 - P_2}{R} = i' + \frac{I}{R}\frac{di'}{dt}. \tag{3}$$

So the flow correction, that is the difference between true inertial flow and resistive flow only, is

$$\Delta i = i' - \frac{P_1 - P_2}{R} = -\frac{I}{R}\frac{di'}{dt}. \qquad (4)$$

The corresponding corrections for the pressure change in the two compartments during time increment, dt, are

$$dP_1 \leftarrow dP_1 - \frac{\Delta i \cdot dt}{C_1} = dP_1 - \frac{1}{C_1}\frac{I}{R}di'$$

and (5)

$$dP_2 \leftarrow dP_2 + \frac{\Delta i \cdot dt}{C_1} = dP_2 + \frac{1}{C_1}\frac{I}{R}di',$$

where, for any time increment, dt , one can compute $di' = \frac{dt}{I}(P_1 - P_2 - Ri')$ from (3), with $i' = \int di'$ starting from the initial conditions of the simulation. Using this approach, pressures in the thoracic aorta and abdominal aorta of the 70 kg adult model were corrected for inertial effects using the values for inertance I indicated in Table S3.2 based upon adult human anatomy, and scaled for individuals of varying body weight.

Table S3.2. Values of inertance for the 70 kg adult model.

Blood column	Inertance (mmHg-sec/L)
Thoracic and abdominal aorta	12
Right atrium and inferior vena cava	3
Two carotid arteries	16
Two jugular veins	8

Chest compression

To drive the model we specified the pressure, P_{chest} , generated in the mediastinum by external compression of the chest as a half sinusoidal wave

$P_{chest} = \max(0,\ P_{max}\sin(2\pi f t))$, for compression frequency, f .

The peak internal pressure in the chest resulting from external compressions was standardized at P_{max} = 60 mmHg. Here, since we are focusing on the problem of optimal rate, we keep the compression force constant for this particular set of simulations. Chest compressions were simulated for 20-second intervals, and an average systemic perfusion

pressure over this interval (mean aortic pressure minus mean right atrial pressure) was taken as a figure of merit reflecting the quality of CPR.

Parameter values

The adult parameters for the circulatory model describing a textbook normal 70 Kg man are summarized in Table S3.3. To model effects of reduced blood volume in arteries and increased blood volume in veins during cardiac arrest and CPR and the non-linear compliances of blood vessels, as described in Online Supplement 2, the normal values of compliance for the thoracic aorta (ao), abdominal aorta (aa), and carotid arteries (car) in Table S3.3 were doubled. The normal values of compliance for the inferior vena cava (ivc), right heart (rh), and jugular veins (jug) in Table S3.3 were halved.

Table S3.3: Numerical values for normal resistances and compliances of the circulatory model for a 70 kg adult.

Resistances, mmHg/(L/sec)	**Compliances, L/mmHg**
R_h 4470	C_{ao} 0.000936
R_c 60	C_{aa} 0.000468
R_a 25	C_{ivc} 0.0234
R_v 25	C_{rh} 0.0145
R_{body} 1704	C_{pump} 0.012
R_{av} 10	**C_{car} 0.000156**
R_{tv} 10	**C_{jug} 0.00936**
R_{ht} 11400	
R_{jug} 30	

To implement the computer model of the present study equations (1) for the specific constants in Table S3.3 and corrected for inertial effects using (5) were solved using Microsoft Visual Basic to perform numerical integration over successive small increments of time, $\Delta t = 0.001$ sec.

Online Supplement 4: representative analysis of a neonatal chest CT

Figure S4.1 below provides an example of the measurements made in preliminary unpublished studies by one of us (AM). The figure shows an axial CT cut of a neonatal chest. Anterior-posterior internal and external chest depth, heart depth, and non-cardiac thoracic tissue depth were measured from such images, as shown. Using these measurements, the remaining internal depth of the chest between the sternum and spine after external compression, was calculated for external compressions depths of 1/4, 1/3 and 1/2 of the back-to-front chest diameter. Over-compression was defined as residual internal chest depth < 10mm. In this example, the internal chest depth represents about 60 percent of external chest depth. If the chest were compressed by 30 percent of the external chest depth, this would take up one half of the volume between the inner aspect of the sternum and the anterior edge of the spine, providing a vigorous compression of the heart. However, if the chest were compressed 50 percent of the external chest depth, the compression would take up 5/6 of the volume between the inner aspect of the sternum and the spine, providing traumatic over-compression of the heart.

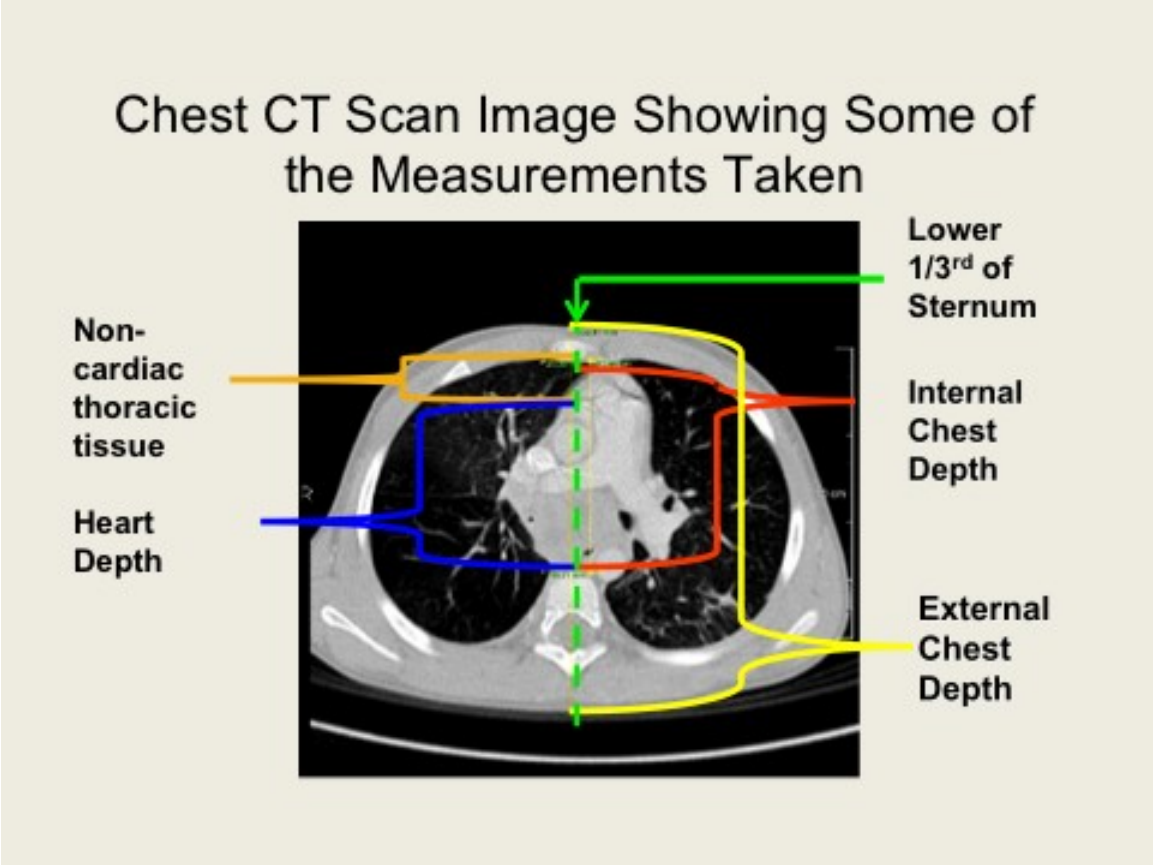

Figure S4.1. Axial CT cut showing dimensions of the neonatal chest used for analysis.